CNRS
Centre National de la Recherche Scientifique

INFN
Istituto Nazionale di Fisica Nucleare

Effects of CITF misalignments on the longitudinal error signals during the CARM offset phase of AdV+.

VIR-0446A-20

Michele Valentini[1, 2*], Julia Casanueva[3], Maddalena Mantovani[3], and Antonio Perreca[1, 2*]

[1] *University of Trento*
[2] *INFN TIFPA*
[3] *European Gravitational Observatory*

Date: November 2, 2020

[*] *corresponding author:* michele.valentini@unit.it

VIRGO* A joint CNRS-INFN Project
Via E. Amaldi, I-56021 S. Stefano a Macerata - Cascina (Pisa)
Secretariat: Telephone (39) 050 752 521 * FAX (39) 050 752 550 * Email: ego@ego-gw.it

Contents

This document reports the simulated behaviour of the "3f" longitudinal error signals against small misalignment of the CITF mirrors during the initial steps of the AdV+ lock acquisition. The aim of the study is to evaluate the necessity of angular controls during this phase.

1 Introduction

- intro: locking sequence overview, used errsigs in carm offset phase
- intro 2: issue: angular misaligment vs long errsigs
- simulation overview: intro and config
- simulation overview: issues and convergence
- results (each signal)
- conclusions

Due to the addition of the signal recycling mirror, the Advanced Virgo Plus locking sequence has been redesigned for O4, in order to take into account of the additional Degree of Freedom (DOF) that has to be controlled.

The design of the new locking sequence is thoroughly explained in [1], but it will be summarised in the following section, since it is useful for the understanding of the study reported in this document.

1.1 AdV+ locking sequence overview

The new locking sequence, thoroughly explained in [1], involves a step in which the arm cavities are locked off-resonance with respect to the main infrared carrier laser. This is performed with the usage of an auxiliary green laser, generated at twice the infrared laser frequency plus an offset given by an AOM. This step is called "CARM offset phase" and allows to minimise the effect of the arm cavities on the infrared carrier beam while locking the Central Interferometer (CITF) DOFs.

An important detail related to the CARM offset phase is that, during this phase, "3f" error signals are used to control the CITF DOFs, as explained in [**?**]. These are signals that are demodulated at a frequency three-times the sideband modulation frequency used for the LSC controls. This is done in order to have error signals that are robust against the "CARM offset reduction", that is the subsequent step in which the arm cavities are brought back to resonance with the main infrared carrier beam. This step does not allow to keep the CITF under locked with the traditional '1f' signals (which are are the results of the beating of the carrier beam with a "first order" sideband), since they are highly affected by the carrier beam phase change that happens when the arms are brought to resonance with it. **??**

Since the main contribution to the '3f' signals is the beating of "first order" sidebands with "second order" ones, not involving the carrier beam, the effect of the carrier phase change on such signals is minimal.

This study will give therefore particular attention to the behaviour of these '3f' signals.

In order to solve this issue, as explained in [**?**], "3f" error signals are instead used, which are signals that are demodulated at a frequency three time the modulation frequency of the ISC sidebands. The main contribution to these signals is instead the beating of "first order" sidebands with "second order" ones, minimising the effect of the carrier phase change on such a signal.

1.2 Misalignment issues during the CARM offset phase

In the current AdV configuration, the angular degrees of freedom controls are engaged in full-bandwidth mode only at the end of the locking sequence.

The influence of misalignment of the CITF mirrors (Input Mirrors, PR mirror, SR mirror) with respect to the longitudinal error signals used during the CARM offset phase has therefore been studied, and the results are reported in the following sections.

A similar study for the PRITF configuration was previously made in [**?**], with a focus on the effects of misalignment of the PR, crucial for the variable finesse technique.

1.3 Simulation details and limits

The simulations have been performed using the modal simulation software Finesse 2 [2].

An overview of the details and limits of the used simulation setup is given in section 2.2 of [**?**]. The main difference between the setup used in this study and the one described in [3] is the removal of the arm cavity end mirrors, which is a simple way emulate the effect of large CARM offset. This simplifies the setup and the simulations by removing the influence of the CARM and DARM DOFs on the carrier beam.

An additional challenge related to the study of misaligned components was the necessity of simulating a large number of Hermite-Gauss modes to correctly represent the laser field in the interferometer.

To optimise the simulation process, the procedure was divided in the following steps:

- Working point optimisation and simulation convergence check;
- simulation of the longitudinal DOFs sweeps;
- optimisation and study of the error signals.

Working point optimisation and simulation convergence check In order to accurately study the behaviour of the interferometer with respect to the misalignment of the CITF suspended mirrors, the correct working points of the CITF DOFs need to be found for each angle of each misaligned mirror. This is accomplished by minimising the '3f' error signals using the built-in 'lock' command of Finesse. The found working points are then saved and used in the next steps.

In addition to this step, the convergence of the simulations has to be tested, i.e. whether the amount of H-G t.e.m. modes used in the simulation is enough to give realistic results. This is performed by finding the CITF working points with an increasingly higher 'maxtem' (that means a larger amount of higher order t.e.m. modes) and comparing the results. Once the relative WP variation between simulations performed with one 'maxtem' value and the two subsequent ones is lower than 1%, the 'convergence' condition is considered satisfied and this 'maxtem' value is then used. To reduce the time required to perform the next simulation steps, this process is performed independently for each simulated angle of each misaligned mirror, since higher misalignment values require a higher 'maxtem' value to obtain a convergence.

E' DAVVERO L'1% ??? ERA PIu SIMILE AD UN 5 MI PARE. controllo sul file

Simulation of the longitudinal DOFs sweeps Once the CITF WPs and the 'maxtem' values have been found for each angle of each misaligned mirror, the longitudinal sweeps can be performed. These sweeps are accomplished by moving the mirrors corresponding to one DOF at a time.

During this step the behaviour of the laser beam in the main interferometer ports is monitored in detail by a large amount of photodiode and amplitude detectors. In particular, both I and Q quadrature of each error signal are acquired, so that the demodulation phase can be optimised in the following step.

Optimisation and study of the error signals This last step involves the use of the results of the simulations performed in the previous step to study the behaviour of the error signals at different values of misalignment of the interferometer.

To accomplish this, the error signal $Err[\phi]$ for each DOF and its optimal demodulation phase ϕ is reconstructed from the I and Q components of the simulated photodiodes as follows:

$$Err[\phi] = \Re[(Err_I + iErr_Q)e^{-i\phi}] \tag{1.1}$$

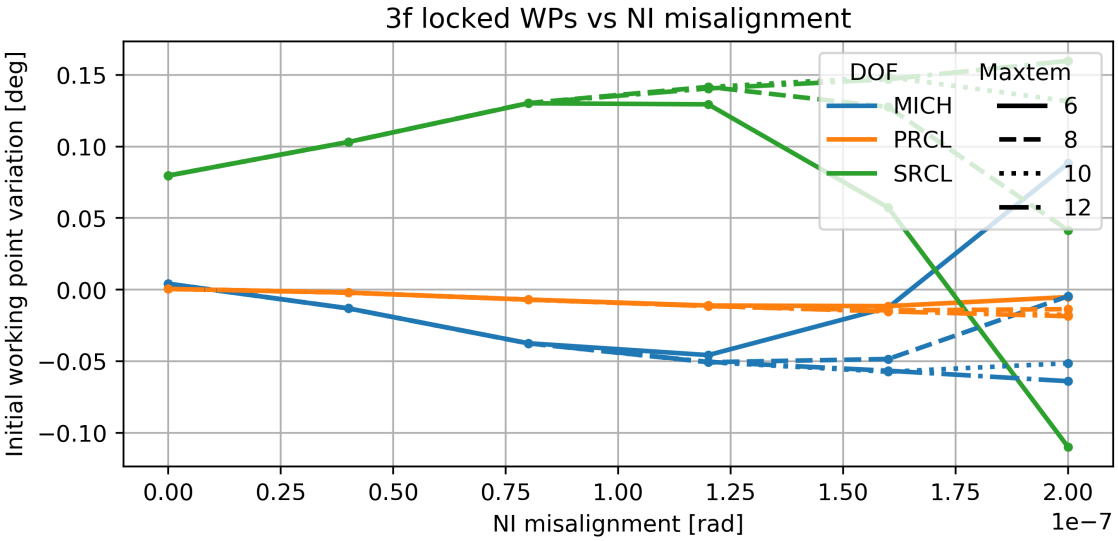

Figure 1: Convergence study of locks vs NI misalignment.

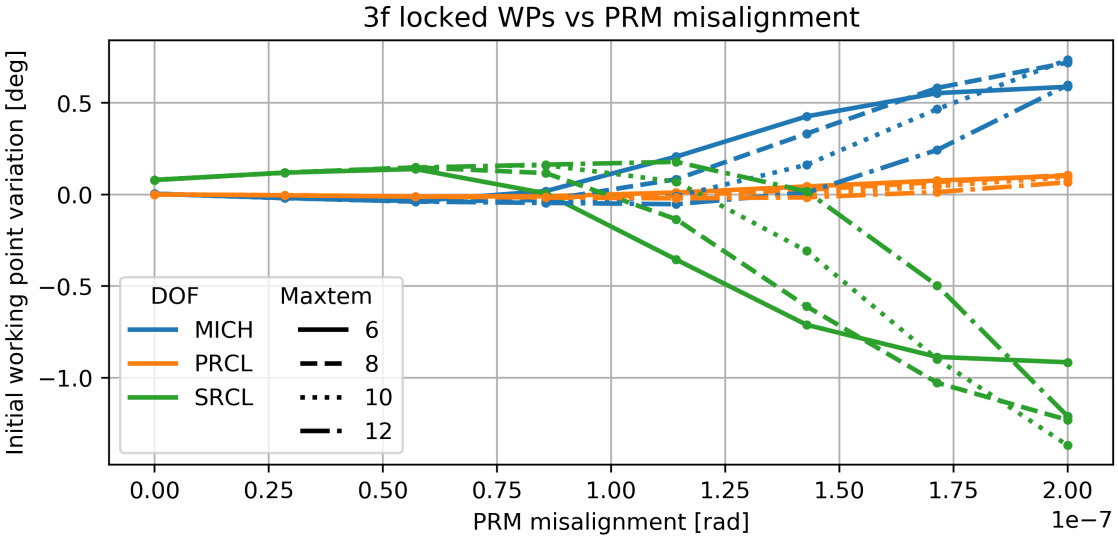

Figure 2: Convergence study of locks vs PR misalignment.

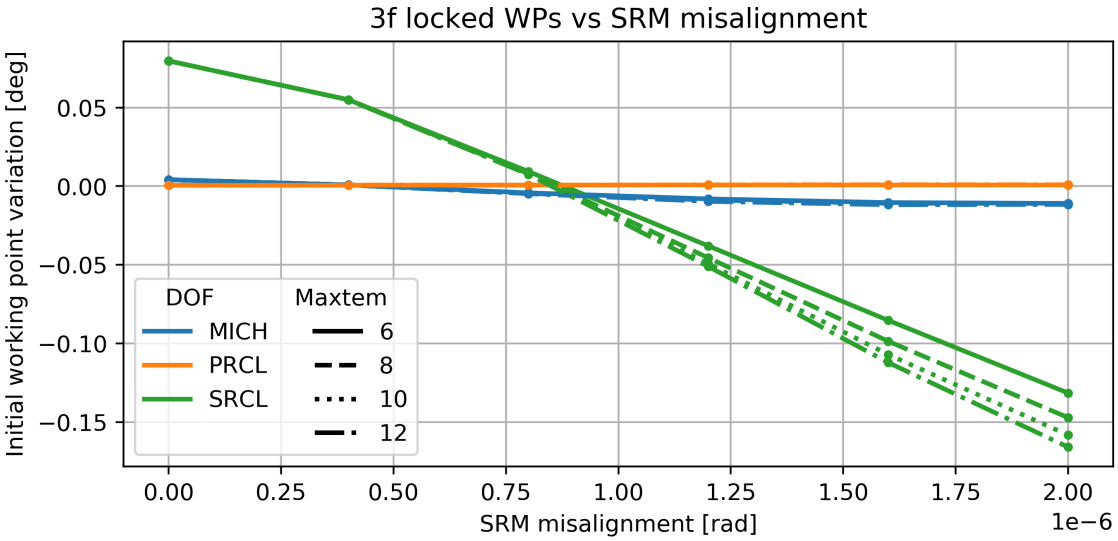

Figure 3: Convergence study of locks vs SR misalignment.

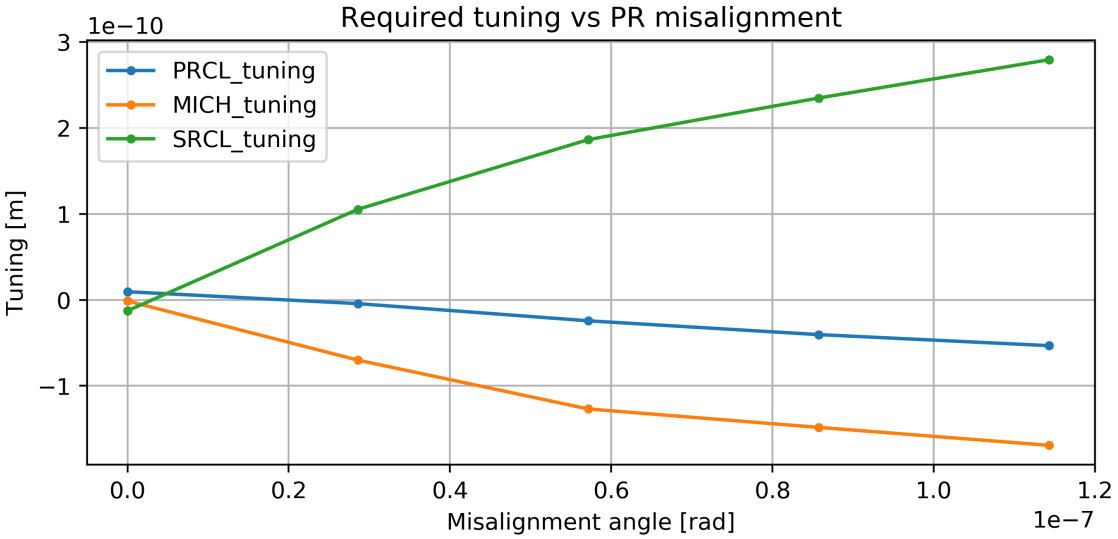

Figure 4: Final CITF working points used in the PR misalignment simulations.

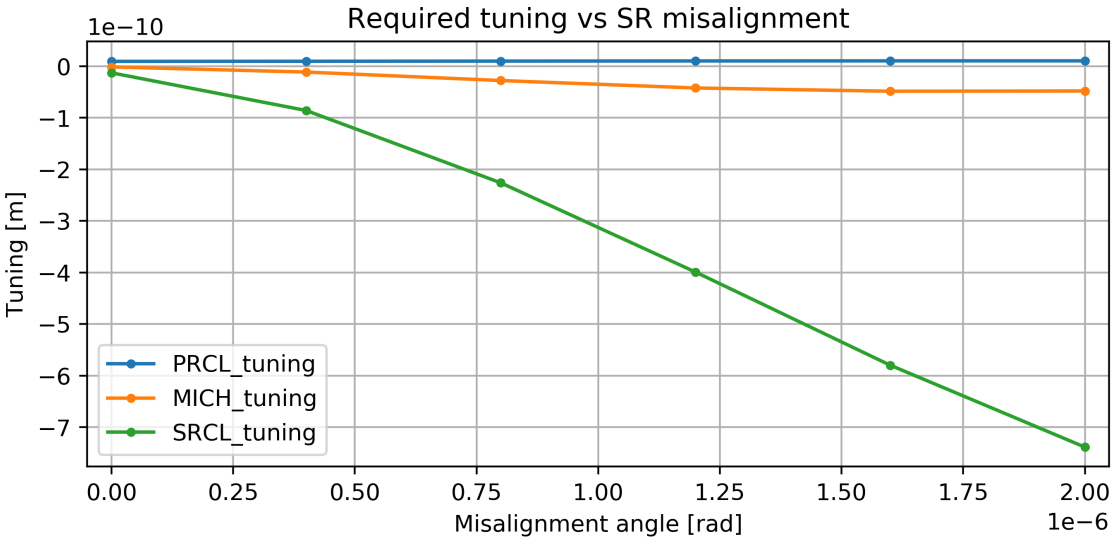

Figure 5: Final CITF working points used in the SR misalignment simulations.

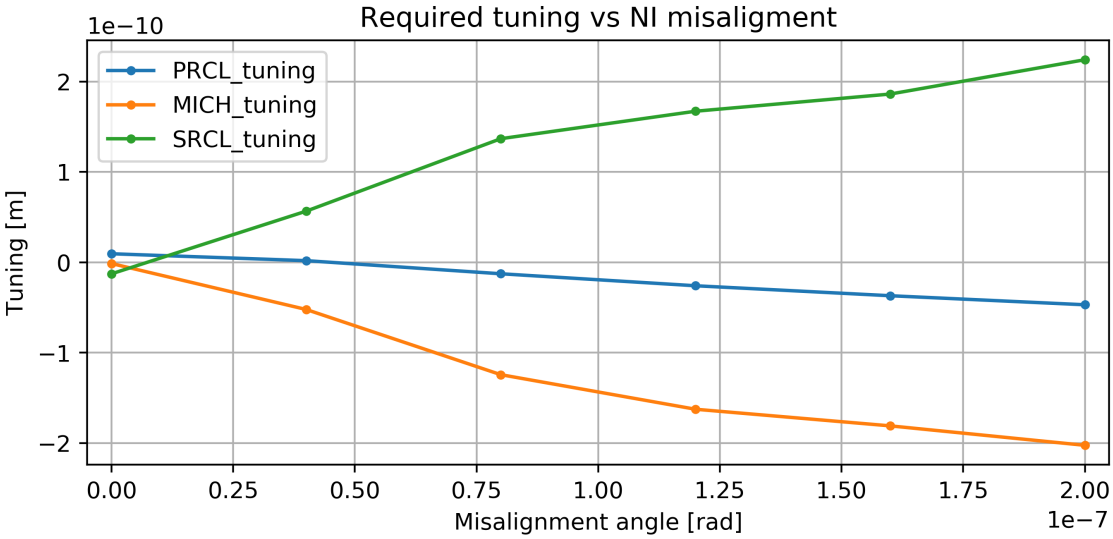

Figure 6: Final CITF working points used in the NI misalignment simulations.

DOF	Errsig	OG
PRCL	B2 6*3 MHz	qew
MICH	B2/B4 56*3 MHz Q	aaa
SRCL	B2/B4 56*3 MHz I	qwe

Table 1: CITF error signals

By setting the demodulation phase to the one used in the perfectly aligned condition, one could study the variation of multiple figures of merit against the misalignment of the CITF optics.

- Optical gains;
- working point;
- shape of the error signal (multiple zero crossings etc).

As discussed in detail in the following chapter, the study of these quantities allows to estimate a "threshold angle" beyond which the error signal cannot be used to keep the CITF locked.

Additionally, we studied how the optimal demodulation phases of each error signal changes with the misalignment, allowing to estimate the increase of cross-couplings between the different DOFs.

2 results

LIST OF SIGNALS

The planned error signals

2.1 different influence of misalignment on different modulation frequencies???

2.2 Optical Gain variation

One of the main effect of the misalignment is a sharp reduction of optical gain on the longitudinal PDH error signals. The extent of this effect depends both on the error signal and on which mirror is misaligned. In particular, simulations allowed to notice that higher frequency signals are less impacted by the misalignment than the lower frequency ones. INSERISCO PLOT DI THRESHOLD VS DEMOD FREQUENCY This is in accordance with the fact that higher frequency sidebands have lower finesse resonance and therefore are less impacted by misalignments and other interferometer non-idealities than lower frequency ones

The amount of gain loss that can be sustained by a loop without losing lock depends on several factors, in particular on the "gain margin" of the involved control loop.

Automatic loop gain tuning processes based on a real-time estimate of the loop Unity Gain Factor (UGF), can help , as long as they "react" quickly enough.

However, empirical experience tells us that an optical gain loss over a factor of 1/2 often leads to loss of control. For this reason the misalignment angle at which this threshold is reached is an important figure of merit subject of this study.

Results:

2.3 working point

Another way in which the misalignment of the central interferometer impacts the LSC error signals is by changing their zero crossing point —> rispetto al vero wp? o cambia anche il vero wp?

RIESCO A MISURARE PICCO PRCL VS WP ERRSIG DI PRCL?

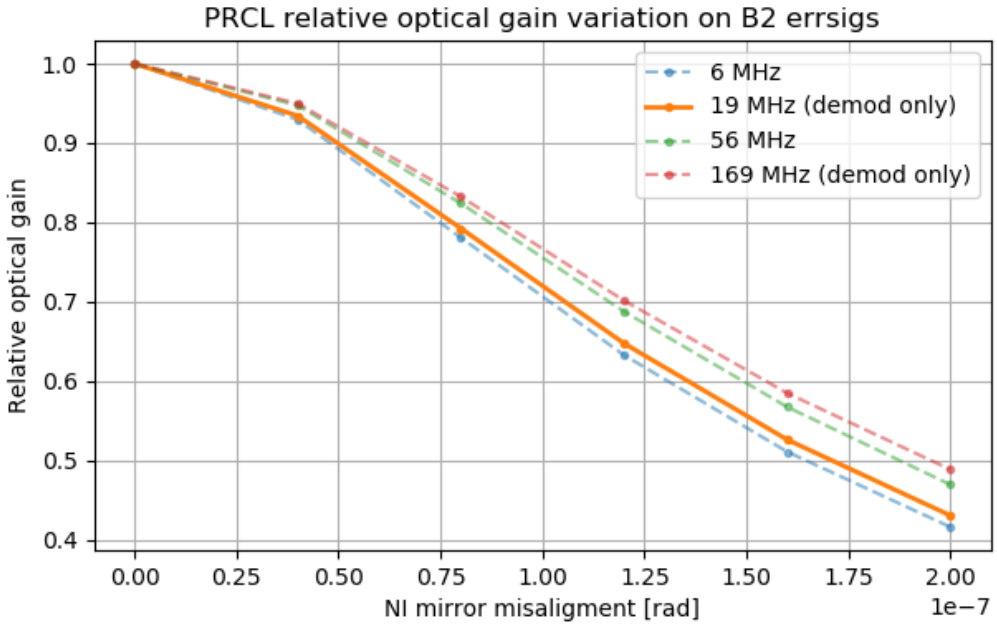

Figure 7: OG variation of B2 signals for PRCL displacement vs NI misalignment. The highlighted line corresponds to the used 3f signal.

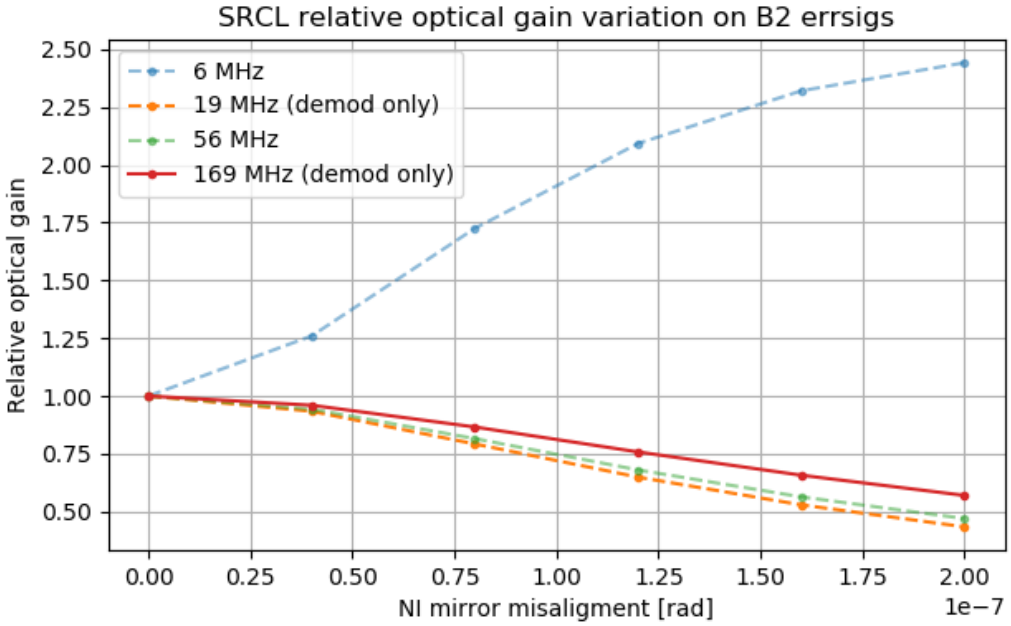

Figure 8: OG variation of B2 signals for SRCL displacement vs NI misalignment. The highlighted line corresponds to the used 3f signal.

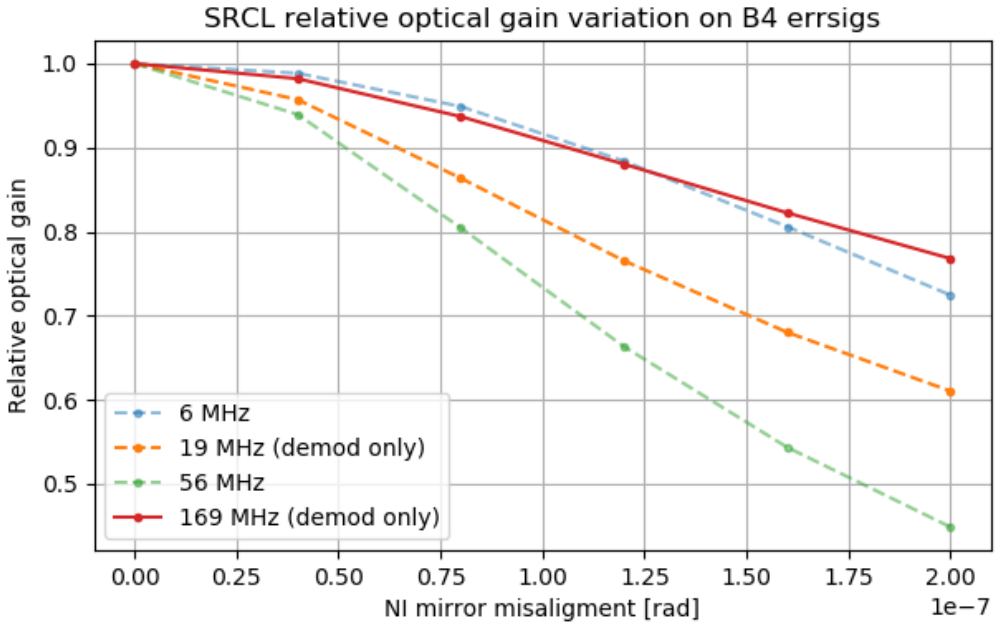

Figure 9: OG variation of B4 signals for SRCL displacement vs NI misalignment. The highlighted line corresponds to the used 3f signal.

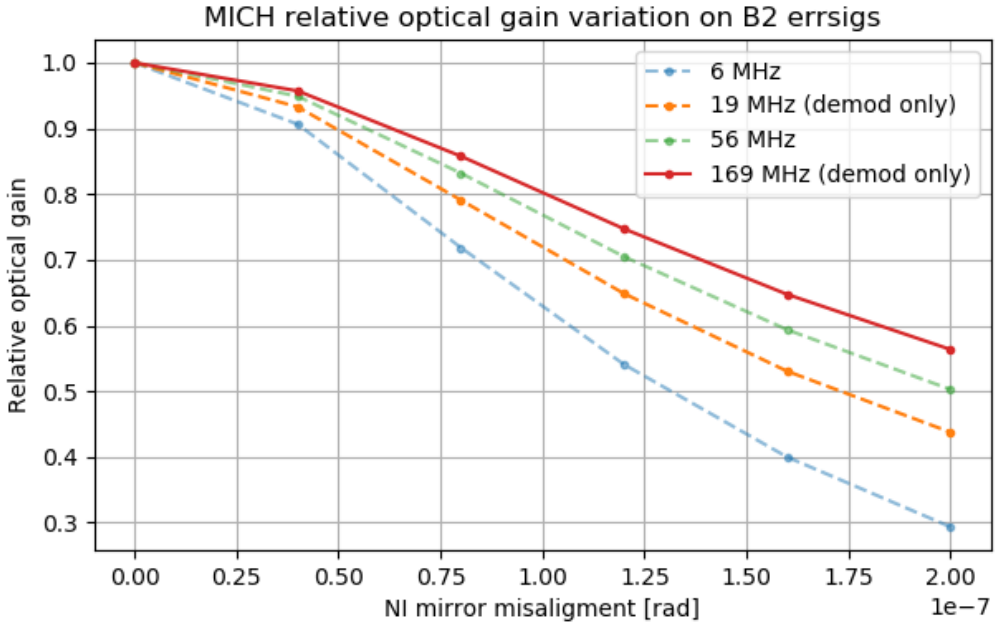

Figure 10: OG variation of B2 signals for MICH displacement vs NI misalignment. The highlighted line corresponds to the used 3f signal.

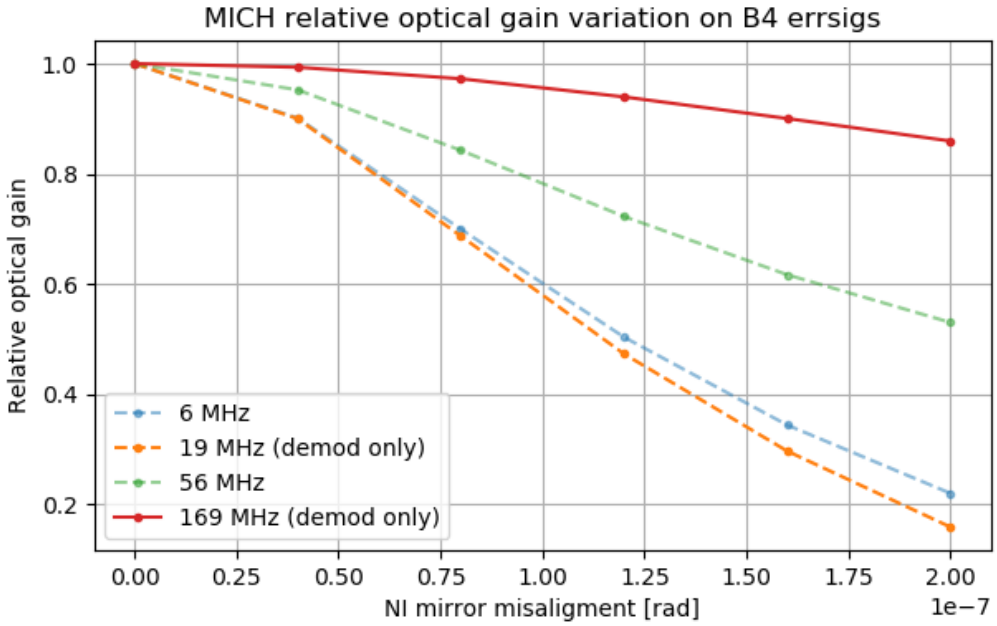

Figure 11: OG variation of B4 signals for MICH displacement vs NI misalignment. The highlighted line corresponds to the used 3f signal.

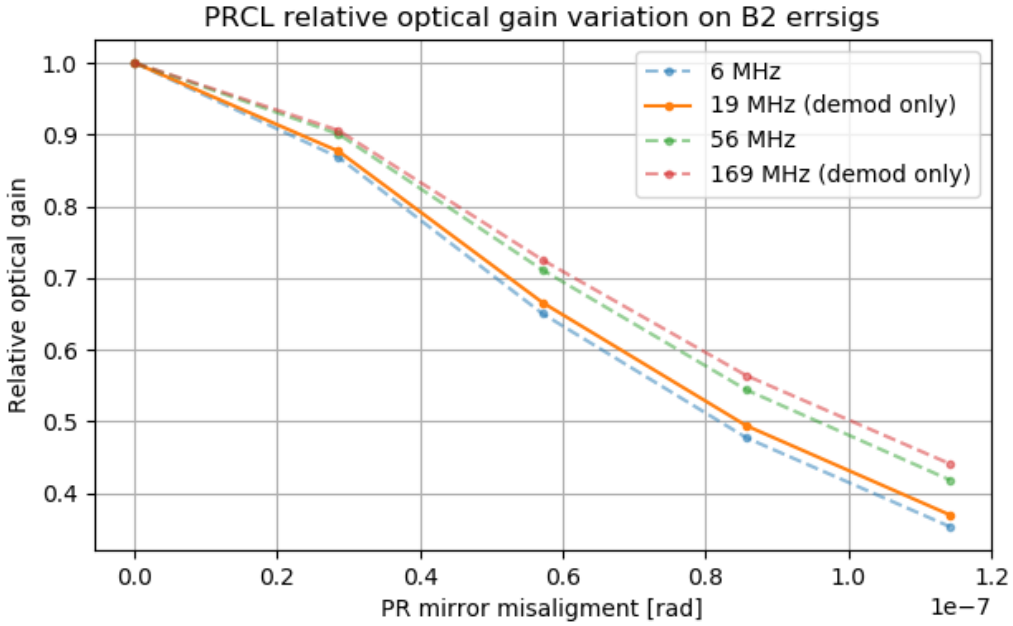

Figure 12: OG variation of B2 signals for PRCL displacement vs PR misalignment. The highlighted line corresponds to the used 3f signal.

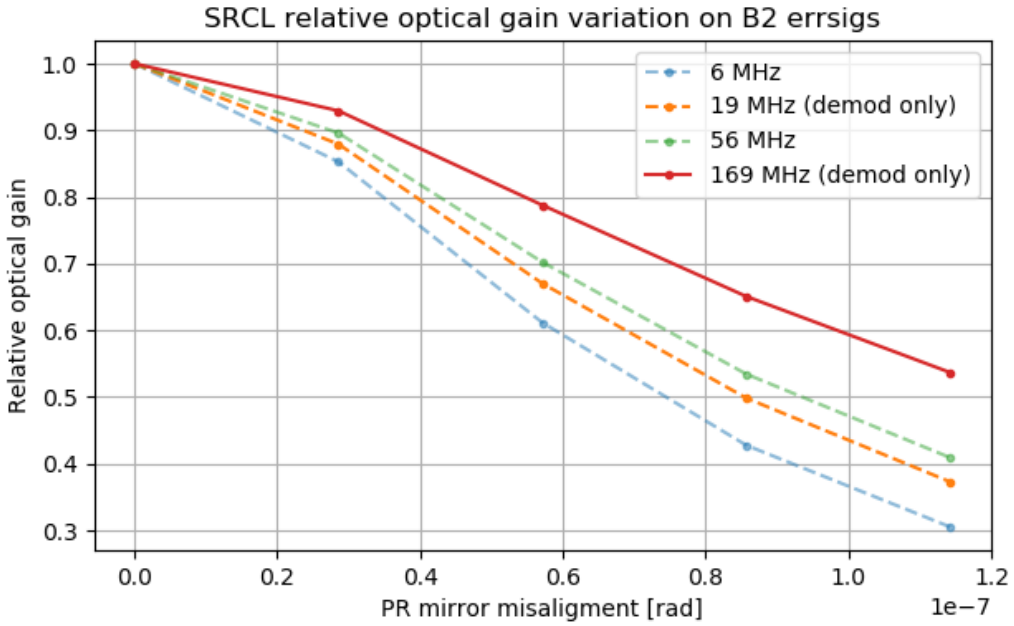

Figure 13: OG variation of B2 signals for SRCL displacement vs PR misalignment. The highlighted line corresponds to the used 3f signal.

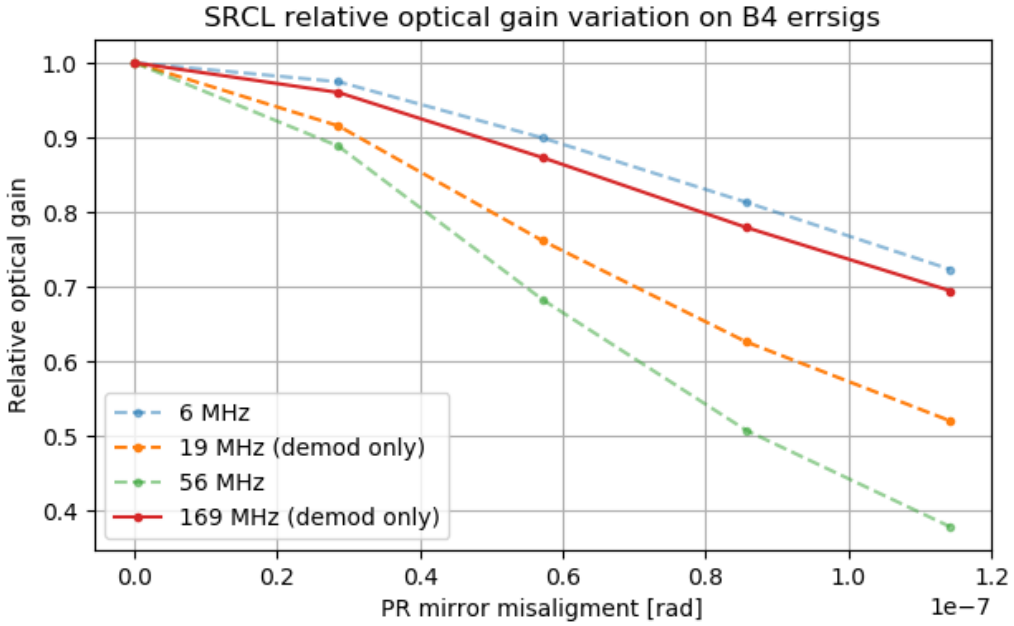

Figure 14: OG variation of B4 signals for SRCL displacement vs PR misalignment. The highlighted line corresponds to the used 3f signal.

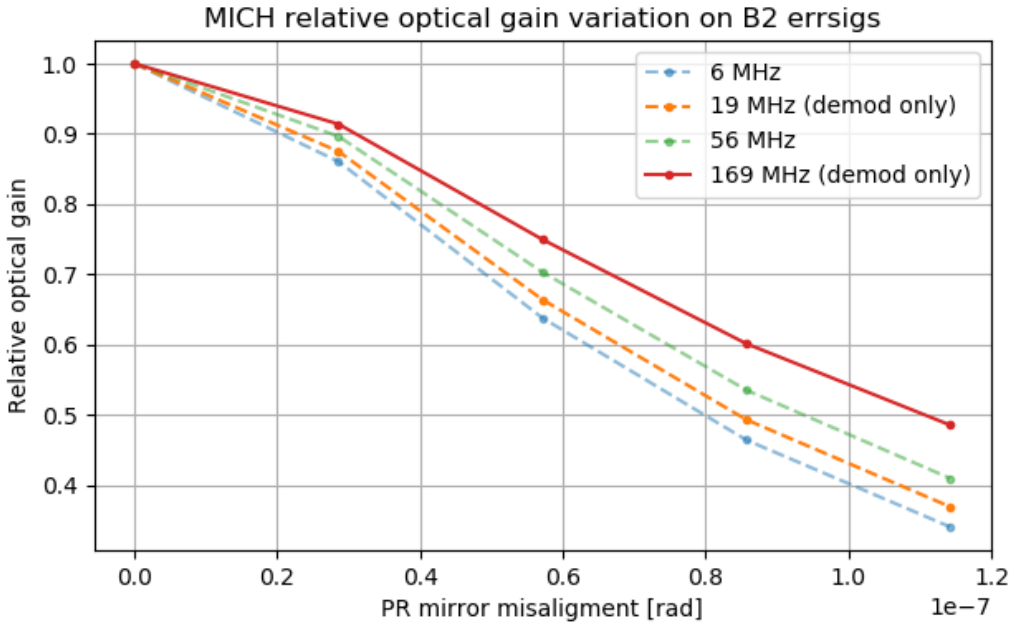

Figure 15: OG variation of B2 signals for MICH displacement vs PR misalignment. The highlighted line corresponds to the used 3f signal.

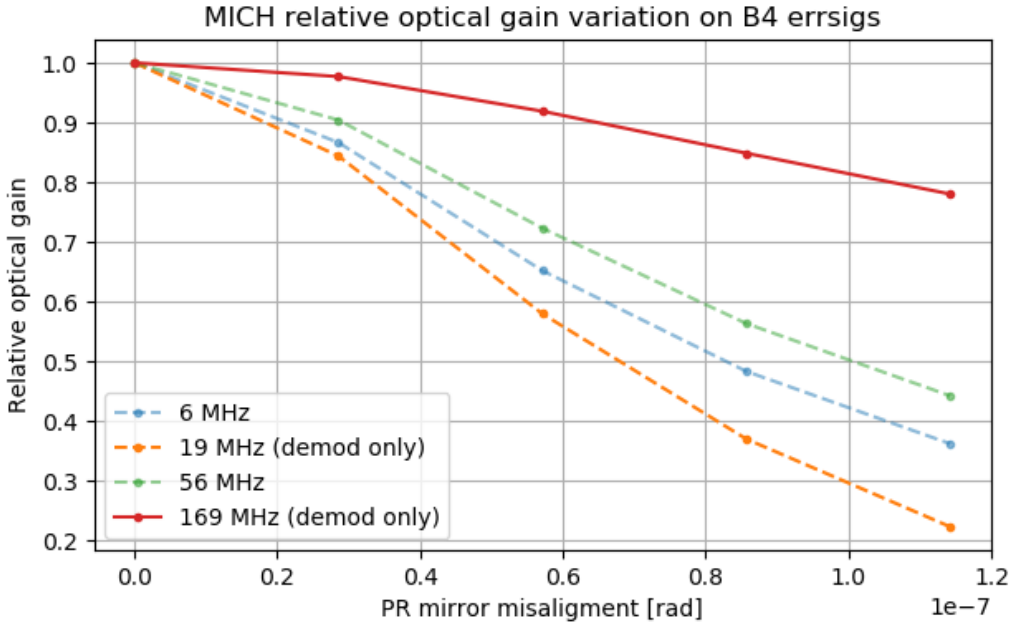

Figure 16: OG variation of B4 signals for MICH displacement vs PR misalignment. The highlighted line corresponds to the used 3f signal.

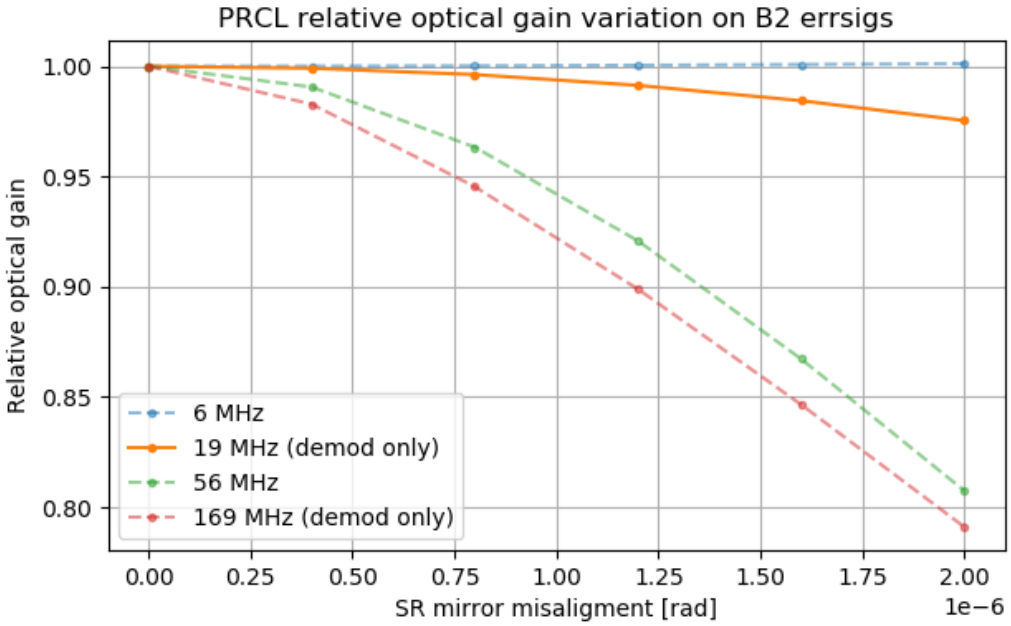

Figure 17: OG variation of B2 signals for PRCL displacement vs SR misalignment. The highlighted line corresponds to the used 3f signal.

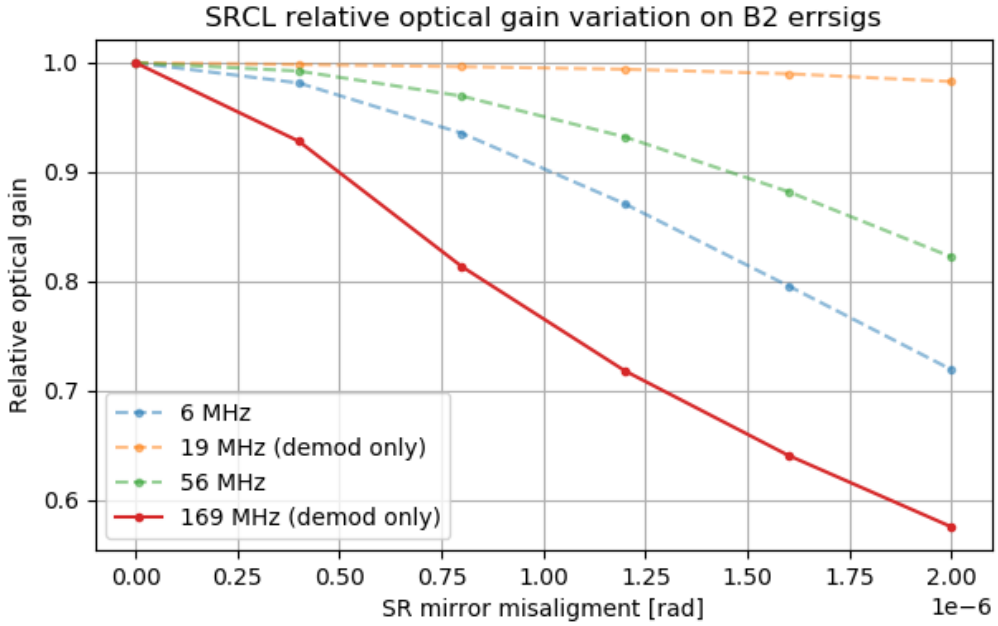

Figure 18: OG variation of B2 signals for SRCL displacement vs SR misalignment. The highlighted line corresponds to the used 3f signal.

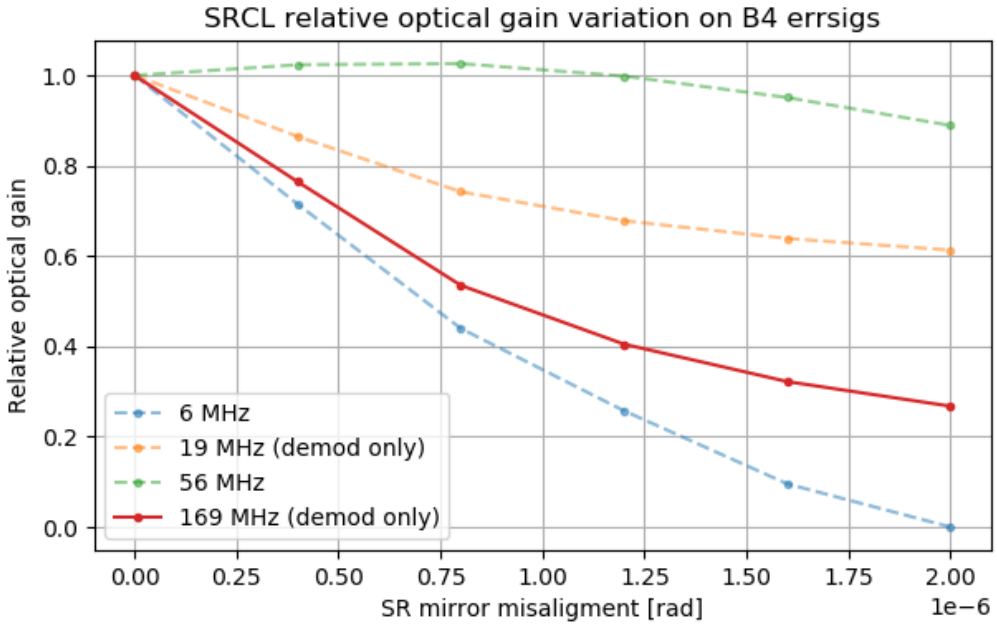

Figure 19: OG variation of B4 signals for SRCL displacement vs SR misalignment. The highlighted line corresponds to the used 3f signal.

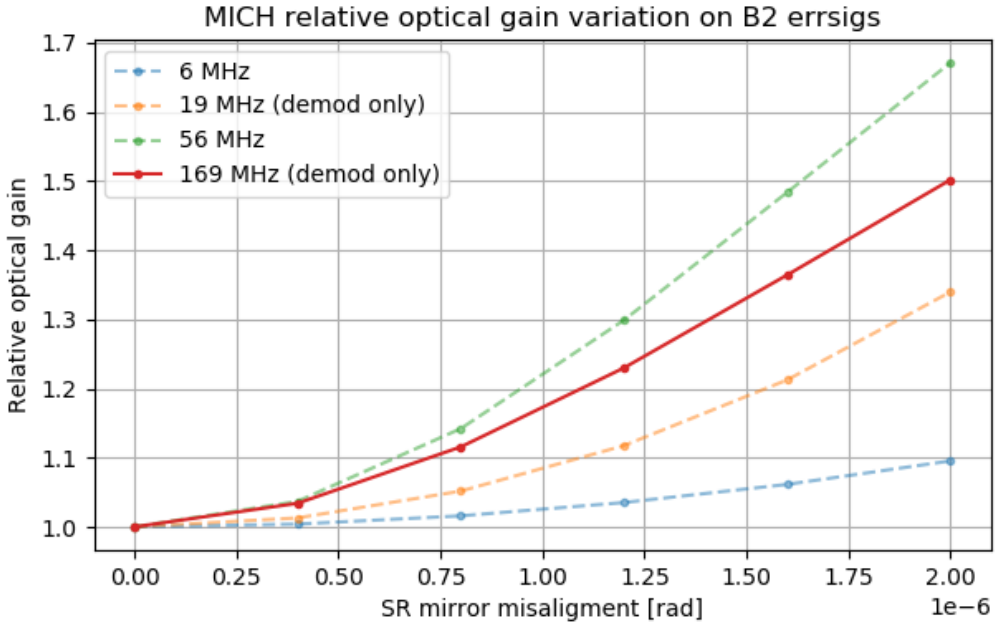

Figure 20: OG variation of B2 signals for MICH displacement vs SR misalignment. The highlighted line corresponds to the used 3f signal.

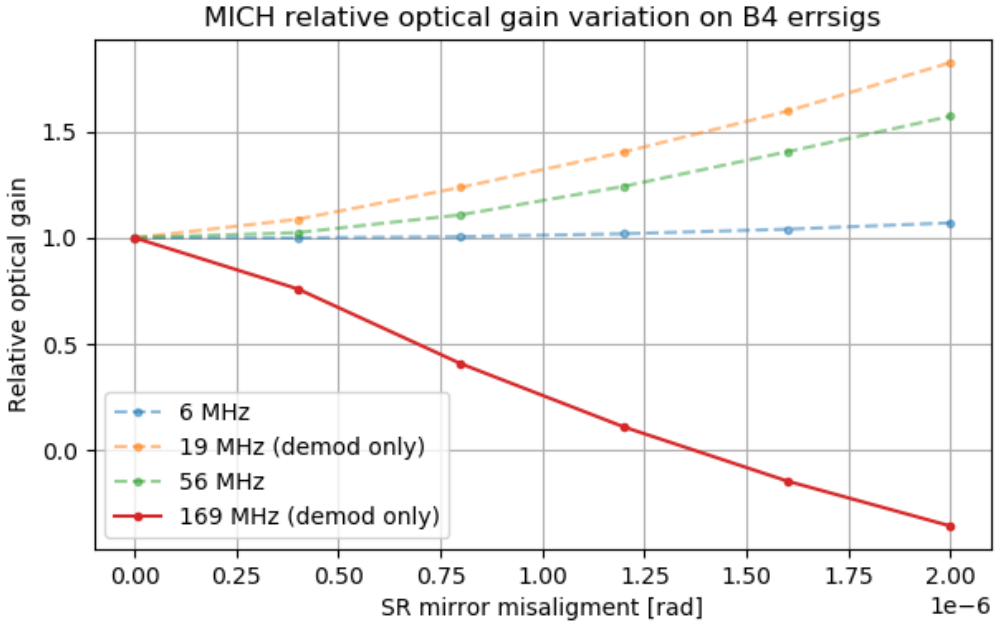

Figure 21: OG variation of B4 signals for MICH displacement vs SR misalignment. The highlighted line corresponds to the used 3f signal.

– overview of 3f signals when aligned

– og variation – add plot with comparison (full misalignment vs no misalignment) – add plot with comparison of 50% thresholds – phi variation – wp variation – coupling??

References

[1] M. Mantovani A. Allocca, A. Chiummo. Locking strategy for the advanced virgo central interferometer. Technical report. VIR-0187A-16. 2

[2] Daniel David Brown and Andreas Freise. Finesse, May 2014. You can download the binaries and source code at http://www.gwoptics.org/finesse. 3

[3] "avirgo_sr_t=0_4_cold.kat". uploaded in Virgo SVN directory ISC/finesse/steadystate https://websvn.ego-gw.it/listing.php?repname=advsw&path=/ISC/finesse/steadystate/. 3